

Feasibility Study of the Pixel Readout TPC Technology at high luminosity Tera Z on CEPC

Yue Chang,^{a,b,c} Huirong Qi,^{b,c,*} Xin She,^{b,c,d} Chunxu Yu,^a Jinxian Zhang,^{b,c} Hongliang Dai,^{b,c} Jian Zhang,^{b,c} Linghui Wu,^{b,c} Guang Zhao,^{b,c} Gang Li,^{b,c} Manqi Ruan,^{b,c} Jianchun Wang^{b,c} and Zhi Deng^e

^aSchool of Physics, Nankai University,
94 Weijin Road, Tianjin, China

^bInstitute of High Energy Physics,
19B Yuquan Road, Beijing, China

^cState Key Laboratory of Particle Detection and Electronics,
19B Yuquan Road, Beijing, China

^dUniversity of Chinese Academy of Sciences,
No.1 Yanqihu East Road, Beijing, China

^eDepartment of Engineering Physics, Tsinghua University,
30 Shuangqing Road, Beijing, China

E-mail: qihr@ihep.ac.cn

In recent years, the requirements of the high spatial resolution and dE/dx for the flavor, Z pole, and Higgs physics in the high-energy physics have been raised. To meet this requirements, the design of high-energy e+e- colliders has been improved the very high luminosity to Tera Z. The Circular Electron Positron Collider (CEPC) is a proposed high-luminosity factory for Higgs and Z pole run, with a the maxim luminosity of $10^{36} \text{ cm}^{-2} \text{ s}^{-1}$. Time Projection Chamber (TPC) is an important detector option for tracking in e+e- collider, which included the high spatial resolution and excellent particle identification (PID) resolution. The Pixel readout TPC technology, known for its low material budget, high occupancy, and good PID capabilities, is developed as a promising option at the Tera Z comparing the classical pad readout TPC technology. By the utilizing cluster counting, the pixel readout can significantly enhance PID resolution. The simulation studies are ongoing at Institute of High Energy Physics, CAS to improve detector performance at the different granularity readout. This paper presents the structure of the pixel readout TPC simulation framework and some preliminary results. The simulation results demonstrate the optimization of the high-granularity readout ($300 \mu\text{m} \sim 500 \mu\text{m}$).

The 2023 European Physical Society Conference on High Energy Physics (EPS-HEP2023)
20-25 August 2023
University of Hamburg, Hamburg, Germany

*Speaker

1. Introduction

The Circular Electron Positron Collider (CEPC [1]) was proposed as a Higgs and high luminosity Z factory (at 91 GeV[2]) in last few years. The detector conceptual design of a updated detector consists of a tracking system, which is a high precision (about $100\mu\text{m}$) spatial resolution Time Projection Chamber (TPC) detector as the main track device in very large 3D volume. The tracking system required the high precision performance requirements, but without power-pulsing not likely as the International Linear Collider (ILC), which leads to additional constraints on detector specifications, especially for the case of the machine operating at the high luminosity Z pole (Tera Z). TPC detection technology requires longitudinal time resolution of about 100ns and the physics goals require Particle Identification Detection (PID) resolution of very good separation power with cluster counting to be considered. The simulation and PID resolution show TPC technology potential to extend Tera Z at the future e+e- collider.

TPC technology utilizes dE/dx for particle identification, primarily for hadrons (π , K, p) and electrons. Using methods like truncated mean or maximum likelihood data analysis, dE/dx resolution typically reaches $<5\%$ [3], making it widely used in previous collider experiments [6]. The traditional pad readout, employs pad units on the order of millimeters (e.g., $1\text{ mm} \times 6\text{ mm}$) for dE/dx measurement via charge summation. Pixel TPC technology, known for its low material budget, high position resolution, high occupancy, precise track reconstruction, and excellent PID resolution, is a focal point for international collaborations such as ECFA and LCTPC [4]. However, this approach's Landau-like electron distribution results in a long tail, hindering the correlation between measured energy loss and particle species. An alternative method, cluster counting(dN/dx), following a narrower Poisson distribution. The dN/dx measurement offers the advantage of mitigating various sources of fluctuations compared to the dE/dx measurement, potentially yielding a resolution that is twice as precise.

When the dimensions of readout units and the electron diffusion during the drift process are smaller than the distance between ionization clusters, a strong correlation emerges in the charge deposition on the readout plane, enabling the reconstruction of ionization clusters. This paper presents a simulation study and its findings centered on primary ionization clusters in a pixel readout TPC. By investigating the properties of primary ionization clusters and their relationship with pixel size, we aim to optimize pixel size and explore how improvements in PID resolution, influenced by dN/dx measurements, can be achieved.

2. TPC Technology for e^+e^- collider

TPC detector comprises two main components: the drift volume and the end-plane. In the drift volume, inert argon-based gas serves as the primary working gas, while the end-plane handles critical functions like electron amplification, charge collection, and signal readout. Figure 1 illustrates the TPC's operation: charged particles entering the chamber ionize the working gas, forming ionization tracks. These tracks drift towards the readout plane due to an electric field along the z-axis. Ultimately, readout detectors at the end-plane collect these tracks after electron avalanche amplification. Typically, a uniform magnetic field of 1-3 Tesla, aligned with the electric field, serves as the primary track detector.

With increasing demands in various experiments, especially in collider physics, precise and stable tracking detectors are essential. For instance, the CEPC requires the TPC to achieve a momentum resolution of $\sigma_{pt}/p_t^2 < 10^{-4} GeV$, including a position resolution of approximately $\sim 100, \mu m$. Simultaneously, as collision luminosity rises in colliders and flavor physics goals at the Z pole are pursued, there is a strong demand for the detector's particle identification capability, which must be less than 3%.

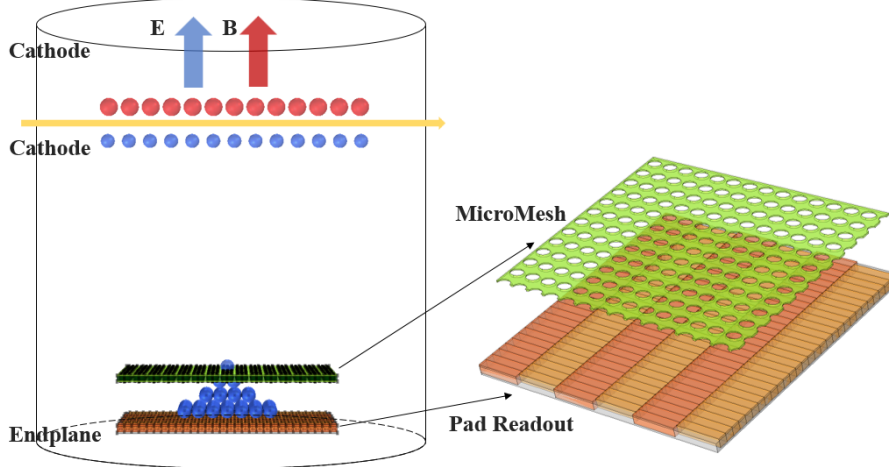


Figure 1: The working principal of TPC.

In recent years, an international collaboration, including CERN RD51 group of the Advanced Gaseous Detector and Electronics Research, has extensively researched TPC readout using Micro Pattern Gaseous Detectors (MPGDs). Various detectors, such as standard GEMs, Micromegas, Resistive Micromegas, THGEMs, and GridPix[5–7], have made significant progress. Researchers worldwide are actively improving TPC detector's performance at the high luminosity. One promising approach is optimizing the readout structure to identify the primary ionization clusters using the high-granularity pad size.

2.1 Pad readout TPC detector

Typically, the Pad readout size is in the range of millimeters, and each individual Pad unit is equipped with dedicated channel to fulfill the counting rate demands of MPGD. The micro-pore structure of MPGD and the typical Pad readout structure are depicted on the right side of Figure 1. The Pad readout structure is commonly designed as a $1 mm \times 6 mm$ strip readout unit, with the long side aligned parallel to the track extension direction.

The resolution $\sigma_{r\phi}^{pad}$ of the pad readout TPC in the $r\phi$ direction towards the boundary of the cylinder chamber in the xy -direction, and the resolution σ_z^{pad} in the z -direction for tracking along the drift length of L, that are described as follows:

$$\sigma_{r\phi}^{pad} = \sqrt{\sigma_{r\phi_0}^{pad2} + \sigma_{r\phi_0}^2 \sin^2(\phi_{track}) + L \frac{D_{r\phi}^2}{N_{eff}} \sin(\theta_{track}) \left(\frac{6mm}{h_{pad}} \right) \left(\frac{3.0T}{B} \right)^2} \quad (1)$$

$$\sigma_z^{pad} = \sqrt{(\sigma_{z0}^{pad})^2 + L(D_z^{pad})^2}$$

where the term ($\frac{6mm}{h_{pad}}$) accommodates the amount of charge (Q_{pad}) collected on the pad, which has a height h_{pad} different from the nominal 6 mm height designed for the TPC detector. In conventional dE/dx detection, charge summation is typically carried out using the center-of-gravity method. This approach is commonly employed across a wide range of experiments, from small to large Pad readout TPC, as illustrated by the following function:

$$R_{dE/dx} = \frac{\sigma_{dE/dx}}{\mu_{dE/dx}} \propto L^{-0.32} \cdot N^{-0.13} = N^{-0.45} \cdot G^{-0.13} \quad (2)$$

In the formula, $R_{dE/dx}$ represents the measured resolution of ionization energy loss. It is evident from the equation that decreasing the size of the readout Pad also contributes to some extent to the enhancement of dE/dx. However, it is important to note that this reduction in Pad size also introduces a more intricate electronic connection system as a corresponding trade-off.

2.2 Pixel readout TPC detector

Pixel readout[8] TPC detector technology employs a micro-electronically system (MEMS) or the bump bonding to process the chip and create a pixel grid for charge digitization. These readout units typically have higher granularity, usually ranging from tens to hundreds of micrometers, enabling precise single-electron cluster detection and improved track resolution. Figure 2 shows an schematic the pixel readout.

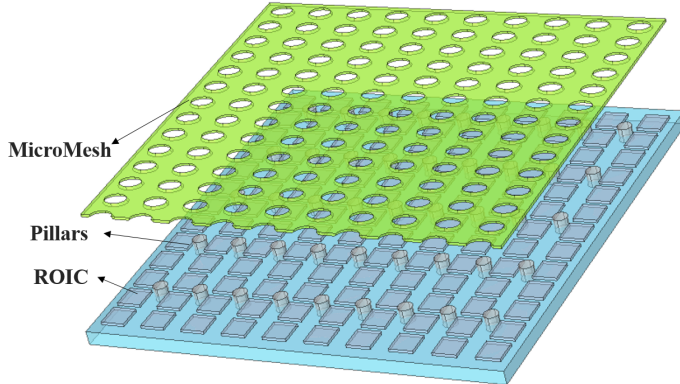


Figure 2: Schematic diagram of pixel readout structure.

The resolutions for the pixel readout TPC in the transverse directions, σ_r^{pixel} and $\sigma_{r\phi}^{pixel}$, as well as the resolution in the longitudinal z-direction for a drift length L, are provided as follows:

$$\begin{aligned} \sigma_r^{pixel} &= \sigma_{rphi}^{pixel} = \sqrt{(\sigma_{rphi_0}^{pixel})^2 + LD_{rphi}^2 \left(\frac{3.0T}{B}\right)^2} \\ \sigma_z^{pixel} &= \sqrt{(\sigma_{z0}^{pixel})^2 + L(D_z^{pixel})^2} \end{aligned} \quad (3)$$

where $\sigma_{r\phi}^{pixel} = 16 \mu m$, which is determined the zero drift length in a 3.0 Tesla magnetic field. $D_{r\phi_0}$ represents the transverse diffusion coefficient of the operational gas (T2K gas) under the influence of the magnetic field and at saturation drift velocity.

Unlike the pad readout, which achieves better resolution when the track aligns with the readout unit extension, square pixel units provide precise track measurements even at angles. Under identical conditions, pixel readout significantly improves momentum resolution by increasing track sampling points. Furthermore, the primary clusters' reduced sensitivity to fluctuations enhances the particle discrimination capability of pixel readout. However, it's worth considering that reducing the pixel readout unit's area allows for single-electron cluster analysis but leads to an increase in channels, data volume, and power consumption.

3. Simulation study of the pixel readout

3.1 Simulation framework

The CEPC Pixel Readout TPC software framework is built using Garfield++[9] and Geant4[10]. The framework consists of two parts: signal digitization and data reconstruction. The digitization part parameterized processes such as primary ionization, drift, diffusion, and amplification at the readout. The data reconstruction includes event finding, track reconstruction, and the assessment of detector performance using cluster counting. This software framework facilitates a comprehensive simulation of particle tracks within the TPC, enabling research into detector performance parameters such as dE/dx and PID during various physical processes.

The geometric parameters of the TPC were adopted from the CEPC TPC design, featuring an inner diameter of 0.3 m and an outer diameter of 1.8 m. The drift distance covers 2.35 m, which equals half the length of the CEPC TPC. A magnetic field of 2 Tesla is applied, and the selected working gas is T2K.

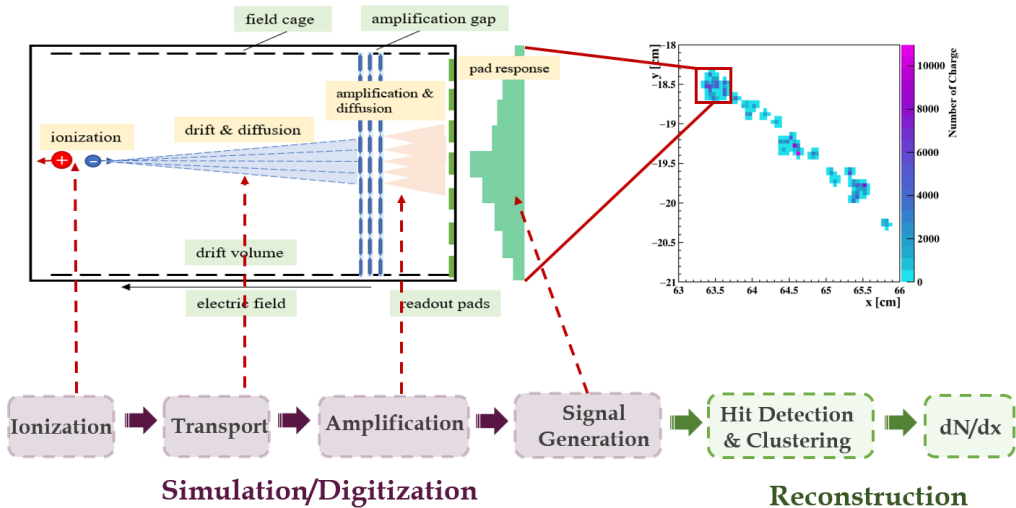


Figure 3: The CEPC Pixel Readout TPC software framework.

3.2 Track simulation under TPC geometry

The simulation of tracks relies on the integrated HEED interface in Garfield++. This interface enables the simulation of primary ionization processes. During the simulation, the Track Heed

function is used to retrieve information such as the count of primary ionization clusters and the distribution of cluster sizes.

Figure 4(a) displays the normalized distribution of ionization clusters along the track of incident particles. Along this track, the distribution of clusters is uniform, providing theoretical evidence for the feasibility of measuring primary ionization clusters. Simulation studies were conducted to examine the number of primary ionization clusters under varying readout unit sizes, as depicted in Figure 4(b). According to the simulation results, when the pixel size is 1, cm in T2K gas, there are 37.4 cl./cm. This aligns with the expected primary ionization count of the minimum ionizing articles in argon-based gas (approximately ~ 30 cl./cm), confirming the model's validity. With a pixel size of 300, μm , the number of primary ionization clusters is 1.2 cl./cm. Consequently, theoretically, when the pixel size is 300 μm , it becomes possible to individually measure each primary ionization cluster. These simulation findings can guide the optimization of pixel sizes to effectively avoid redundant electronic channels and minimize power consumption.

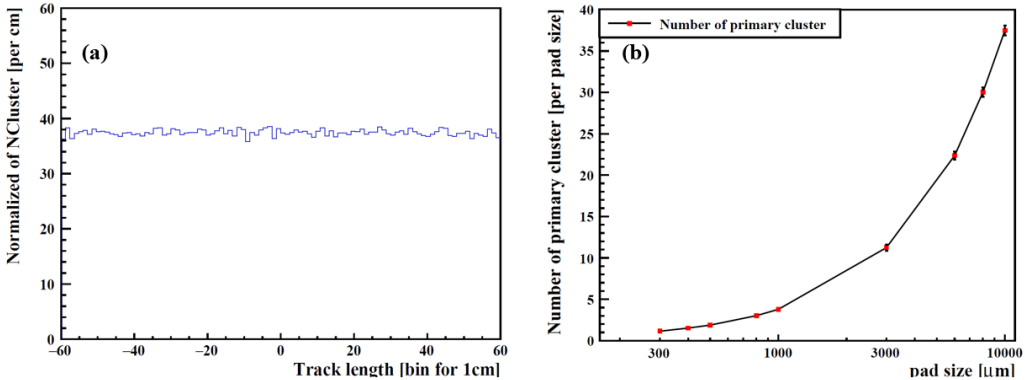


Figure 4: Normalized results of ionization cluster distribution along the track (a); Variation in primary ionization cluster count with pixel sizes (b).

To enhance our comprehension of the particle discrimination capabilities of pixel readout technology, we investigated the number of primary ionization clusters for various types and momentum of the incident particles. The particle separation power (S_{AB}) for distinguishing between two distinct particle types is formulated as follows:

$$S_{AB} = \frac{|\mu_A - \mu_B|}{\sqrt{\frac{1}{2}(\sigma_A^2 + \sigma_B^2)}} \quad (4)$$

According to equation (4), the particle separation power is directly proportional to the difference in average ionization. Figure 5 (a) displays the number of primary ionization cluster for K and π at various momentum. At 5 GeV/c, the separation power between these two particles reaches 7.5σ (with $\sigma \sim 0.8$).

Conversely, Figure 5 (b) presents the separation power among different particles, including K , π , p and e . It's important to note that these results are based on the count of primary ionization clusters. In practical scenarios, factors such as diffusion and electronics may reduce the detection efficiency of cluster counting, and it may not achieve 100%. Nonetheless, the advantages of cluster counting remain evident, significantly advancing research in the field of flavor physics.

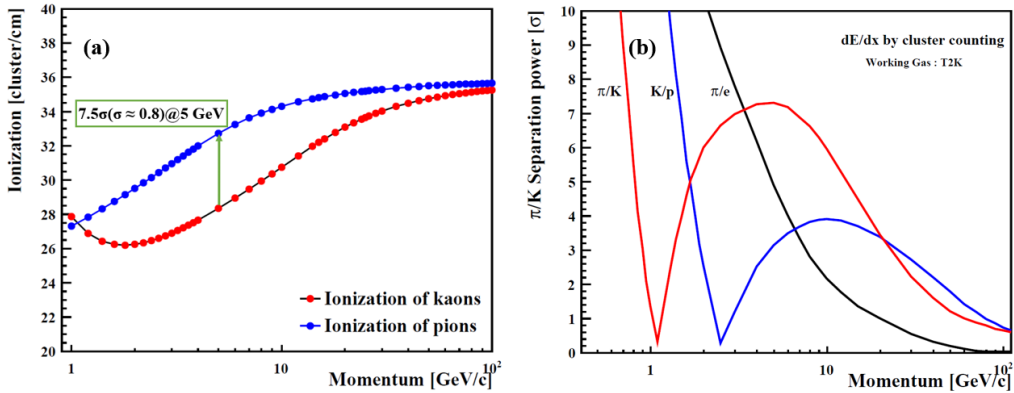


Figure 5: Ionization density of K and π particles at different momentum in T2K Gas (a); Particle separation power among multiple particle types: K , π , p , and e (b).

3.3 Some simulation results

Based on the previous discussion and simulation results, if the size of the readout unit and the diffusion during the electron drift process are smaller than the distance between ionization clusters, then the charge depositions obtained on the readout plane will exhibit strong correlations and allow for the reconstruction of ionization clusters. Due to the substantial drift distance in large TPC, the impact of diffusion cannot be overlooked, and therefore, the method of cluster counting cannot achieve 100% detection efficiency.

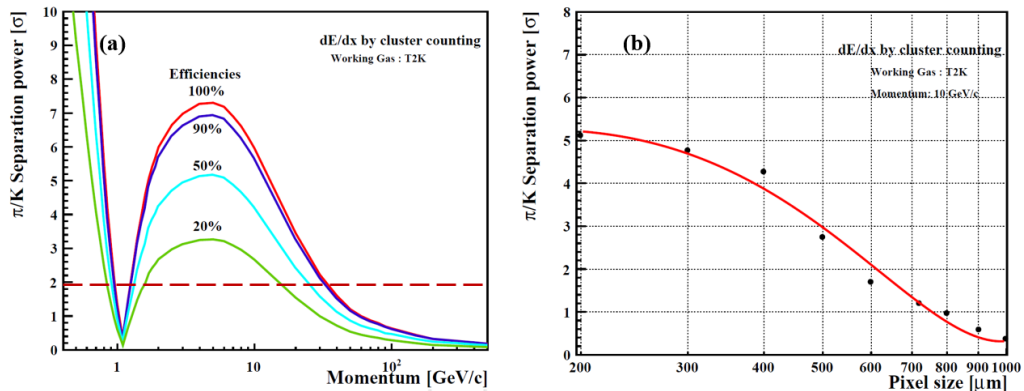


Figure 6: The PID resolution of π and K using the cluster counting method under varying detection efficiencies. The red dotted line represents the typical PID resolution achieved by the charge summation method (a); The impact of pixel size on separation power for π and K particles (b).

In Figure 8(a), the particle discrimination capability achievable using cluster counting methods at different efficiencies has been analyzed. The red dotted line in the figure represents the typical PID resolution achievable with charge summation methods (typically 2σ). It can be observed that for particles with momentum in the range of 2-20 GeV/c, even at a detection efficiency as low as 20%, the particle separation power using cluster counting methods remains higher than that of charge summation methods.

Figure 8(b) illustrates the relationship between the separation power of π , K and pixel size, with results based on pixel hit counts at the end-plane, considering the impact of diffusion. The drift distance is set at 50 cm, and the drift distances from each point on the track to the end-plane are equal. This simulation result indicates that when the pixel size falls within the range of 300 μm to 500 μm , it can potentially provide more than a twofold improvement in PID resolution. Furthermore, with the incorporation of reconstruction algorithms within the subsequent software framework, this result will undergo further optimization and enhancement.

4. Conclusion

A software simulation framework dedicated to the study of pixel readout technology has been established. This framework is designed for investigating the properties of primary ionization clusters, analyzing the advantages of pixel readout technology in particle discrimination, and optimizing pixel sizes while ensuring detector performance. Based on simulations conducted within this software framework, it has been demonstrated that employing pixel readout for cluster counting can offer a potential improvement of at least two-fold when the pixel size falls within the range of 300 μm to 500 μm . Ongoing work involves the development of reconstruction algorithms, which are expected to further enhance particle discrimination capabilities when the new function will be integrated into the framework.

References

- [1] João Barreiro Guimarães da Costa, Yuanning Gao, Shan Jin, Jianming Qian, Christopher G Tully, Charles Young, Lian-Tao Wang, Manqi Ruan, Hongbo Zhu, Mingyi Dong, et al. Cepc conceptual design report: Volume 2-physics & detector. 2021.
- [2] Wenhao Xia, Jie Gao, Yiwei Wang, and Dou Wang. Cepc z-pole polarization design studies. *International Journal of Modern Physics A*, 36(22):2142003, 2021.
- [3] R Abbasi, Yasser Abdou, M Ackermann, J Adams, JA Aguilar, M Ahlers, D Altmann, K Andeen, J Auffenberg, X Bai, et al. An improved method for measuring muon energy using the truncated mean of dE/dx . *Nuclear Instruments and Methods in Physics Research Section A: Accelerators, Spectrometers, Detectors and Associated Equipment*, 703:190–198, 2013.
- [4] Jochen Kaminski, LCTPC collaboration, et al. Tpc development by the lctpc collaboration for the ild detector at ilc. In *Journal of Physics: Conference Series*, volume 2374, page 012149. IOP Publishing, 2022.
- [5] C Ligtenberg, K Heijhoff, Y Bilevych, K Desch, H van der Graaf, F Hartjes, J Kaminski, PM Kluit, G Raven, T Schiffer, et al. Performance of a gridpix detector based on the timepix3 chip. *Nuclear Instruments and Methods in Physics Research Section A: Accelerators, Spectrometers, Detectors and Associated Equipment*, 908:18–23, 2018.
- [6] D Attié, M Batkiewicz-Kwasniak, P Billoir, A Blanchet, A Blondel, S Bolognesi, D Calvet, MG Catanesi, M Cicerchia, G Cogo, et al. Characterization of resistive micromegas detectors

- for the upgrade of the t2k near detector time projection chambers. *Nuclear Instruments and Methods in Physics Research Section A: Accelerators, Spectrometers, Detectors and Associated Equipment*, 1025:166109, 2022.
- [7] M Cortesi, S Rost, W Mittig, Y Ayyad-Limonge, D Bazin, J Yurkon, and A Stolz. Multi-layer thick gas electron multiplier (m-thgem): A new mpgd structure for high-gain operation at low-pressure. *Review of Scientific Instruments*, 88(1), 2017.
 - [8] Michael Lupberger. The pixel-tpc: A feasibility study. In *2015 IEEE Nuclear Science Symposium and Medical Imaging Conference (NSS/MIC)*, pages 1–1. IEEE, 2015.
 - [9] Rob Veenhof. Garfield, a drift chamber simulation program. In *Conf. Proc. C*, volume 9306149, pages 66–71. World Scientific, 1993.
 - [10] John Allison, Katsuya Amako, John Apostolakis, Pedro Arce, Makoto Asai, Tsukasa Aso, Enrico Bagli, A Bagulya, S Banerjee, GJNI Barrand, et al. Recent developments in geant4. *Nuclear instruments and methods in physics research section A: Accelerators, Spectrometers, Detectors and Associated Equipment*, 835:186–225, 2016.